A FINITE ELEMENT METHOD FOR THE ACTIVE CARDIAC MUSCLE

J. Ohayon[1], C. Bourdarias[2], S. Gerbi[2] and C. Oddou[3]

1. ABSTRACT

A finite element modelling for large deformations response of active, incompressible, nonlinear elastic and transversely isotropic soft tissue is presented. A new constitutive law describing the mechanical properties of the active muscle during the whole cardiac cycle is proposed. Three-dimensional finite elements were used to obtain solutions to a free active contraction and uniaxial extension of a rectangular sample assuming negligible body forces and inertia. The problems were chosen for the existence of analytical solutions for finite element model validation.

2. INTRODUCTION

Few FE studies for active myocardium have been developed for ventricular wall stress analysis [1, 2]. In the previous works, the active stress tensor is not derived from a time-dependent strain energy function, but is written as an unidirectional time-dependent tension in the fiber direction. The purposes of this paper are to: (i) formulate an active three-dimensional material law for a nonlinear hyperelastic, transversely isotropic and incompressible continuum medium, which allows us to describe continuously the cardiac cycle by using time-dependent activation functions, (ii) derive the related three-dimensional FE and (iii) test the accuracy and convergence of the proposed numerical methods.

Keywords: Constitutive law, Finite element method, Active tissue, Hyperelasticity, Anisotropic material

---

[1] Professor, Dept. of Composite Materials, Engineering School of Chambéry ESIGEC, France

[2] Assistant Professor, Dept. of Mathematics, Université de Savoie, Chambéry, France

[3] Professor, Dept. of Mechanics and Physics, Université Paris Val-de-Marne, Créteil, France

3. THE MECHANICAL MODEL AND ITS VARIATIONAL FORMULATION

3.1 Constitutive law for the active cardiac tissue

To be consistent with our mathematical formulation, the letter $\mathbf{\Phi}$ is used for non elastic gradient tensor and the letter $\mathbf{F}$ is used for elastic gradient tensor. The activation of the muscle fibers changes the properties of the material and at the same time contracts the muscle itself. To have a continuous elastic description during the activation of the myocardium, we used an approach similar to the one proposed by Ohayon and Chadwick [3], Taber [4]. From its passive zero-stress state P, the activation of the muscle fibers is modeled by two transformations (Fig. 1).

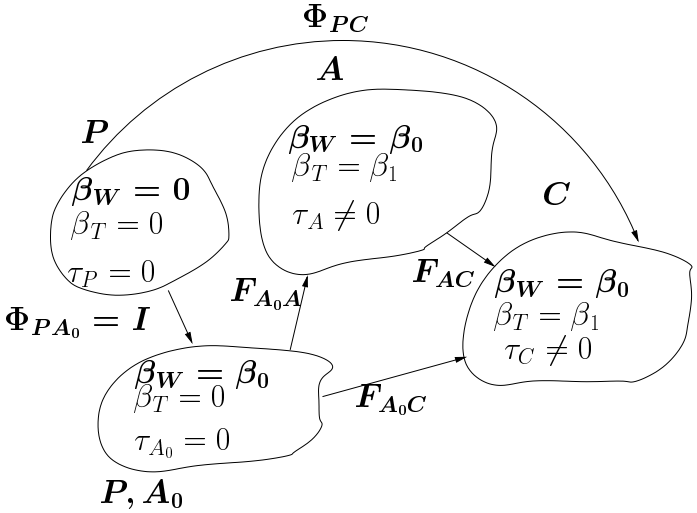

Figure 1

The first one (from state P to virtual state A_0) changes the material properties without changing the geometry, and the second one (from A_0 to A) contracts the muscle without changing the properties of the material. Thus, the former is not an elastic deformation and is described by the gradient tensor $\mathbf{\Phi}_{PA_0} = \mathbf{I}$ where $\mathbf{I}$ is the identity matrix. In that first transformation, only the strain energy function is modified using an activation function $\beta_W(t)$, where t is the cardiac cycle time. The second transformation is an elastic deformation caused by the active tension delivered by the fibers and is described by the gradient tensor $\mathbf{F}_{A_0A}$. Finally, external loads are applied to state A deforming the body through $\mathbf{F}_{AC}$ into C. Thus the global transformation from state P to state C is a non elastic transformation ($\mathbf{\Phi}_{PC} = \mathbf{F}_{A_0C}\mathbf{\Phi}_{PA_0}$), but can be treated mathematically as an elastic one because $\mathbf{\Phi}_{PC} = \mathbf{F}_{A_0C}$. The change of the material properties of the myocardium during the cardiac cycle is described by a time-dependent strain-energy function per unit volume of state P noted $W(\mathbf{E}_{PH}, t)$:

$$W(\mathbf{E}_{PH}, t) = W_{pas}(\mathbf{E}_{PH}) + \beta_W(t) W^f_{act}(\mathbf{E}_{PH}) \tag{1}$$

where $\mathbf{E}_{PH}$ is the Green's strain tensor at an arbitrary state H calculated from the zero strain state P (the state H could be one of the states A_0, A or C shown in figure 1), W_{pas} represents the contribution of the surrounding collagen matrix and of the passive fiber components, W^f_{act} arise from the active component of the embedded muscle fibers, and $\beta_W(t)$ is an activation function equal to zero at end-diastolic state and equal to one at end-systolic state ($0 \leq \beta_W(t) \leq 1$). The last term

of the right side of the equation gives the variation of the mechanical muscle fibers properties during the cardiac cycle. We treat the myocardium as a homogeneous, incompressible and hyperelastic material transversely isotropic with respect to the local muscle fiber direction. This last direction is characterized in an arbitrary state H by the unit vector $\mathbf{f}_H$. In this study, the strain-energy function is [5]

$$\begin{array}{rcl} W_{pas} & = & \frac{a}{b}\left(e^{b(I_1-3)}-1\right)+\frac{a_f}{b_f}\left(e^{b_f(I_4-1)}-1-b_f(I_4-1)\right) \\ W_{act} & = & \frac{c_f}{d_f}\left(I_4+\frac{1}{I_4}-2\right)^{d_f} \end{array} \tag{2}$$

where a, b, a_f, b_f, c_f, d_f are material constants and I_1, I_4 are two strain invariants given by $I_1(\mathbf{E}_{PH}) = tr\,\mathbf{C}_{PH}$ and $I_4(\mathbf{E}_{PH}) = \mathbf{f}_P \cdot \mathbf{C}_{PH}\mathbf{f}_P$ where $\mathbf{C}_{PH}$ is the right Cauchy-Green strain tensor ($\mathbf{C}_{PH} = 2\mathbf{E}_{PH} + \mathbf{I}$). Note that I_4 is directly related to the fiber extension λ_f ($I_4 = \lambda_f^2$).

To incorporate the active contraction, an active fiber stress $T^{(0)}$ was applied in the deformed fiber direction $\mathbf{f}_C$ [1, 2] Hence, during the cardiac cycle, the Cauchy stress tensor in state C (noted τ_C) is given by

$$\boldsymbol{\tau}_C = -p_C\mathbf{I} + \mathbf{\Phi}_{PC}\frac{\partial W\left(\mathbf{E}_{PC},t\right)}{\partial \mathbf{E}_{PC}}\mathbf{\Phi}_{PC}^T + \beta_T(t)T^{(0)}\mathbf{f}_C \otimes \mathbf{f}_C \tag{3}$$

where p_C is the Lagrangian multiplier resulting of the incompressibility of the material [6], and the symbol $\otimes$ denotes the tensor product. The maximal active tension $T^{(0)}$ exists also in the expression of the active strain energy proposed by Lin and Yin [7] and could be identified to the constant $2C_5^a$ (see Eq.(3) in Lin and Yin [7]). The active tension $\beta_T(t)\,T^{(0)}$ is drived by the activation function $\beta_T(t)$ equal to zero at end-diastolic state and equal to one at end-systolic state ($0 \leq \beta_T(t) \leq 1$).

3.2 Variational formulation

The undeformed body state P contains a volume V bounded by a closed surface $\mathcal{A}$, and the deformed body state is, as before, noted C. The corresponding position vectors, in cartesian base unit vectors, are $\mathbf{R} = Y^R\mathbf{e}_R$ and $\mathbf{r} = y^r\mathbf{e}_r$, respectively. However, we write the equations with suitable curvilinear systems of world coordinates noted Θ^A in the reference configuration (state P) and θ^α in the deformed configuration (state C). In this paper we use the same conventional notations for vectors, tensors and coordinates systems than Costa et al. [8], where: (i) capital letters are used for coordinates and indices of tensor components associated to state P, and lower case letters are related to state C, and (ii) $\mathbf{G}$ and $\mathbf{g}$ are the base vectors in states P and C, respectively, for which parenthetical superscript indicates the associated coordinate system (for example $\mathbf{G}_I^{(x)} = \partial\mathbf{R}/\partial X^I = \mathbf{R}_{,I}^{(x)}$ and $\mathbf{g}_i^{(x)} = \partial\mathbf{r}/\partial x^i = \mathbf{r}_{,i}^{(x)}$).

The Lagrangian formulation of the virtual works principle is given by [6]

$$\int_V P^{IJ}\Phi_J^{\cdot\alpha}\nabla_I(\delta u_\alpha)\,dV = \int_V \rho(b^\alpha - \gamma^\alpha)\delta u_\alpha\,dV + \int_{A_2}\mathbf{s}.\boldsymbol{\delta}\mathbf{u}\,dA \tag{4}$$

where P^{IJ} are the components of the second Piola-Kirchhoff stress tensor $\mathbf{P}$ referred to the base tensor $\mathbf{G}_I^{(x)} \otimes \mathbf{G}_J^{(x)}$, $\Phi_I^{\cdot\alpha} = \partial\theta^\alpha/\partial X^I$ are the components of the

gradient tensor $\mathbf{\Phi}_{PC}$ in the base tensor $\mathbf{g}_\alpha^{(\theta)} \otimes \mathbf{G}^{(x)I}$, $\boldsymbol{\delta}\mathbf{u} = \delta u_\alpha \mathbf{g}^{(\theta)\alpha}$ is an arbitrary admissible displacement vector, $\nabla_I(\delta u_\alpha) = \partial \delta u_\alpha / \partial X^I - \mathbf{g}_{\alpha,I}^{(\theta)} \cdot \mathbf{g}^{(\theta)\beta} \delta u_\beta$ are the components of the covariant differentiation vector $\boldsymbol{\delta}\mathbf{u}$ in the base vectors $\mathbf{g}^{(\theta)\alpha}$ (i.e. $\nabla_I(\delta u) = \nabla_I(\delta u_\alpha)\mathbf{g}^{(\theta)\alpha}$). The previous differentiation is done with respect to the locally orthonormal body coordinates (X^I, $I = 1, 2, 3$) which coincide with the local muscle fiber direction in state P. The material density in the undeformed body state P is ρ, $\mathbf{b} = b^\alpha \mathbf{g}_\alpha^{(\theta)}$ is the body force vector per unit mass, $\boldsymbol{\gamma} = \gamma^\alpha \mathbf{g}_\alpha^{(\theta)}$ is the acceleration vector, $\mathbf{s}$ is the surface traction per unit area of $\mathcal{A}$, and A_2 is the part of $\mathcal{A}$ not subject to displacement boundary conditions. The Lagrangian formulation for incompressibility is given by

$$\int_V \left(\det g_{IJ}^{(x)} - 1 \right) \, q \, dV = 0 \tag{5}$$

where $g_{IJ}^{(x)}$ is the metric tensor and q is an arbitrary admissible pressure. Eqs.(4)-(5) represent the variational formulation of a system of nonlinear partial differential equations.

4. RESULTS

Through this paper we use a three dimensional finite element with Lagrange trilinear interpolation for the displacements and uniform pressure [9] to compute an approximate solution of Eqs.(4)-(5) on a rectangular mesh, where we neglect the acceleration and body forces ($\mathbf{b} = 0$, $\boldsymbol{\gamma} = 0$). We simulate the loading of a thin sample of myocardium ($1.0 \times 1.0 \times 0.1$ cm^3) in which the fibers are uniformly oriented in one direction Y_1. The coefficents involved in the energy equations (2) are [5]: $a = 0.81$ kPa, $b = 1.5$, $a_f = 1.08$ kPa, $b_f = 2$, $c_f = 55$ kPa, $d_f = 1.8$, and $T^{(0)} = 6,14$ kPa. All the stresses presented in the numerical results are the physical Cauchy stresses (noted σ_{ij}). Note that for reasons of symmetry, in the following simulations, we solve only for a quarter of the sample with appropriated kinematic boundary conditions.

4.1 Passive and active uniaxial tests

This section is devoted to the numerical simulation of an uniaxial extension of the material. This simulation is a common experimental protocol for mechanical tissue testing. These cases are performed by applying equal forces at the nodes of the two opposites element edges. For the uniaxial test in the fiber direction we set $\sigma_{11} \neq 0$, $\sigma_{22} = \sigma_{33} = 0$. For the uniaxial test in the cross-fiber direction we set $\sigma_{11} = 0$, $\sigma_{22} \neq 0$, $\sigma_{33} = 0$. Figure 2 show a very good agreement between the exact and the computed solutions obtained for the passive state ($\beta_W = \beta_T = 0$) and for the active state ($\beta_W = \beta_T = 1$). More precisely in both cases the L^2 norm of the error is less than 10^{-12}. One can see that in the passive and active simulations the fiber direction is significantly stiffer than the cross fiber one.

4.2 Free contraction tests

These cases are performed without applying any displacements or forces at the node of the four element edges, but just by activated the medium. In this simulation,

we set $\sigma_{11} = \sigma_{22} = \sigma_{33} = 0$. These computations are made when the change of rheology occurs ($\beta_W(t) = \beta_T(t) = \sin^2(\pi t)$), which corresponds to real states, or for the virtual states ($\beta_W(t) = 0$ and $\beta_T(t) = \sin^2(\pi t)$). This last case simulates the contraction of the specimen without change of material properties which may occur in some particular biological tissues or pathologies. We present in figure 3, the comparison between the exact and the computed solution in the passive and active states. Again the L^2 norm of the error is less than 10^{-12}.

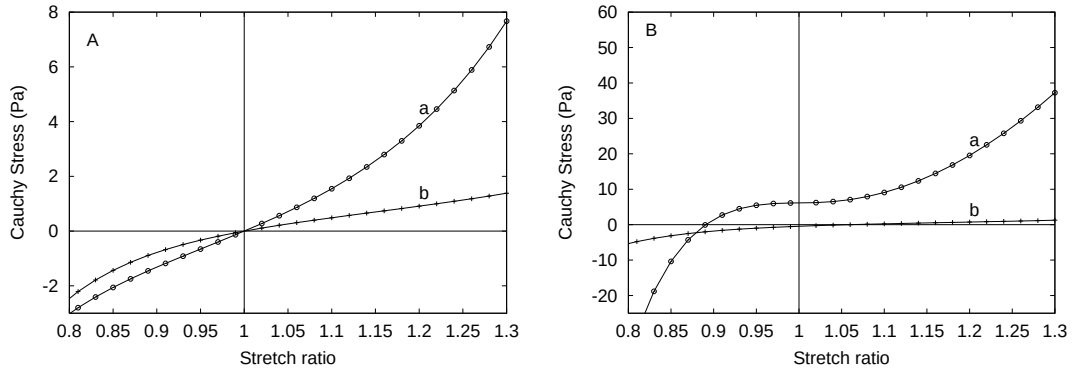

Figure 2: Stress-stretch relations in the fiber direction (curves a) and cross fiber direction (curves b). The lines are the analytical values and the symbols are the computed ones. A- Passive uniaxial tests. B- Active uniaxial tests.

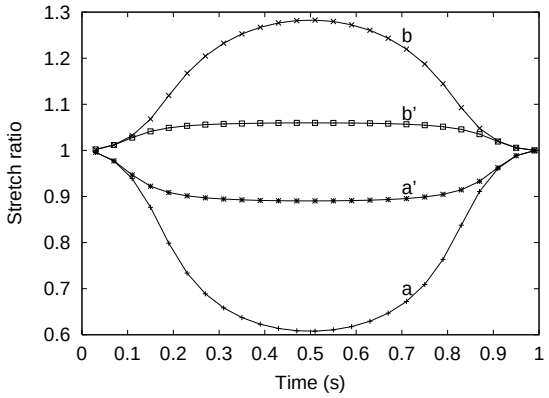

Figure 3: Time evolution of the stretch ratio during free contraction tests of a thin myocardium sample. Results with the assumption of no change of rheology ($\beta_W = 0$, $\beta_T(t) = \sin^2(\pi t)$) in the fiber direction (curve a) and in the cross fiber direction (curve b). Simulation of a more realistic case ($\beta_W(t) = \beta_T(t) = \sin^2(\pi t)$) in the fiber direction (curve a') and in the cross fiber direction (curve b'). The lines are the analytical values and the symbols are the computed ones.

5. CONCLUSION

Based on the work of Costa et al. [8] done on the passive myocardium, we have derived the FE equation for the active soft tissue. This present work is the first implementation of a recently proposed active material law for the myocardium, including the time-dependent strain energy function during muscle contraction, in a

numerical simulation technique. The formulation used a three-dimensional cartesian FE, which has been successfully tested by comparing the numerical and exact or approximate analytical solutions for a variety of quasi-static equilibrium problems in finite elasticity assuming negligible body forces. This model may serve as one of the basic adjustment mechanism of living tissue to the various combinations of loads in the fiber and cross-fiber directions, which prevail in some biological tissue. This FE method has been developed for large deformations of active cardiac tissue and other incompressible, nonlinear elastic, active, anisotropic materials. Thus, several features are incorporated specifically for active ventricular myocardium, but may be useful for a variety of applications in soft tissue biomechanics, such as pathological blood vessels with hypertension. This numerical tool may be adapted for large scale problems such as modeling the heart or artery, by the use of an element by element method on a parallel computer.

REFERENCES

1. P.H.M. Bovendeerd, T. Arts, J.M. Huyghe, D.H. van Campen, and R.S. Reneman. Dependance of local left ventricular wall mechanics on myocardial fiber orientation: a model study. *J. Biomech.*, 25:1129–1140, 1992.
2. A.D. McCulloch, L.K. Waldman, J. Rogers, and J. Guccione. Large scale finite element analysis of the beating heart. *Crit. Rev. Biomed. Eng.*, 20:427–449, 1992.
3. J. Ohayon and R.S. Chadwick. Effects of collagen microstructure on the mechanics of the left ventricle. *Biophys. J.*, 54:1077–1088, 1988.
4. L.A. Taber. On a nonlinear theory for muscle shells: Part II- Application to the beating left ventricle. *J. Biomech. Eng.*, 113:63–71, 1991.
5. J. Ohayon, H. Cai, P.S. Jouk, Y. Usson, and A. Azancot. A model of the structural and functional development of the normal human fetal left ventricle based on a global growth law. *Comp. Meth. Biomech. & Biomed. Engin.*, 5(2):113–126, 2002.
6. L. E. Malvern. *Introduction to the mechanics of a continuous medium.* Prentice-Hall, 1969.
7. D.H.S. Lin and F.C.P. Yin. A multiaxial constitutive law for mammalian left ventricular myocardium in steady-state barium contracture or tetanus. *J. Biomech. Eng.*, 120:504–517, 1998.
8. K.D. Costa, P.J. Hunter, J.S. Wayne, L.K. Waldman, J.M. Guccione, and A.D. McCulloch. A three-dimensional finite element method for large elastic deformations of ventricular myocardium: Part I - Cylindrical and spherical polar coordinates. *ASME J. Biomech. Eng*, 118:452–463, 1996.
9. R. Glowinsky and P. Le Tallec. *Augmented lagrangian and operator-splitting methods in nonlinear mechanics.* SIAM, Philadelphia, PA, 1989.